Article

Development of a Novel Anti-CD44 Variant 8 Monoclonal Antibody C44Mab-94 against Gastric Carcinomas

Hiroyuki Suzuki [1,2,*,#], Nohara Goto [1,#], Tomohiro Tanaka [1], Tsunenori Ouchida [2], Mika K. Kaneko [1,2] and Yukinari Kato [1,2,*]

[1] Department of Molecular Pharmacology, Tohoku University Graduate School of Medicine, 2-1 Seiryo-machi, Aoba-ku, Sendai 980-8575, Japan; s1930550@s.tsukuba.ac.jp (N.G.); tomohiro.tanaka.b5@tohoku.ac.jp (T.T.); k.mika@med.tohoku.ac.jp (M.K.K.)

[2] Department of Antibody Drug Development, Tohoku University Graduate School of Medicine, 2-1 Seiryo-machi, Aoba-ku, Sendai 980-8575, Japan; tsunenori.ouchida.d5@tohoku.ac.jp (T.O.)

* Correspondence: hiroyuki.suzuki.b4@tohoku.ac.jp (H.S.); yukinari.kato.e6@tohoku.ac.jp (Y.K.); Tel.: +81-22-717-8207 (H.S. & Y.K.)

# contributed equally to this work

Abstract: Gastric cancer (GC) is the third leading cause of cancer-related deaths worldwide. GC with peritoneal metastasis exhibits a poor prognosis due to the lack of effective therapy. A comprehensive analysis of malignant ascites identified the genomic alterations and significant amplifications of cancer driver genes, including *CD44*. CD44 and its splicing variants are overexpressed in tumors, and play crucial roles in the acquisition of invasiveness, stemness, and resistance to treatments. Therefore, the development of CD44-targeting monoclonal antibodies (mAbs) is important for GC diagnosis and therapy. In this study, we immunized mice with CD44v3–10-overexpressed PANC-1 cells and established several dozens of clones that produce anti-CD44v3–10 mAbs. One of the clones (C44Mab-94; IgG_1, kappa) recognized the variant-8-encoded region and peptide, indicating that C44Mab-94 is a specific mAb for CD44v8. Furthermore, C44Mab-94 could recognize CHO/CD44v3–10 cells, oral squamous cell carcinoma cell line (HSC-3), or GC cell lines (MKN45 and NUGC-4) in flow cytometric analyses. C44Mab-94 could detect the exogenous CD44v3–10 and endogenous CD44v8 in western blotting and stained the formalin-fixed paraffin-embedded gastric cancer cells. These results indicate that C44Mab-94 is useful for detecting CD44v8 in a variety of experimental methods and is expected to the application of GC diagnosis and therapy.

Keywords: CD44 variant 8; monoclonal antibody; gastric cancer; flow cytometry; immunohistochemistry

1. Introduction

Gastric cancer (GC) is the third leading cause of cancer-related deaths globally [1]. The GC incidence is higher in Eastern Asia than in Western countries [1]. The vast majority of GC are adenocarcinomas, which can be divided into intestinal-type gastric cancer (IGC), diffuse-type gastric cancer (DGC), and mixed histology according to the Lauren classification [2]. The World Health Organization classifies gastric adenocarcinomas into papillary, tubular, mucinous, and poorly cohesive carcinomas [3]. Furthermore, next-generation sequencing defined four molecular subtypes, including Epstein–Barr virus-positive, microsatellite instability, genomically stable, and chromosomally unstable types [4]. The analysis also revealed the alterations in the GC genome and provided treatment options with anti-human epidermal growth factor receptor 2 (HER2) therapy [5] or immune checkpoint inhibitor therapy [6]. However, the benefit of those therapies is limited to a small subset of patients. In patients with advanced GC, especially those with DGC, peritoneal metastasis and subsequent development of malignant ascites are the most frequent cause of death.

Preprints (www.preprints.org) | NOT PEER-REVIEWED | Posted: 15 May 2023 doi:10.20944/preprints202305.0995.v1

Tanaka *et al.*, therefore, performed a comprehensive multi-omic analysis of malignant ascitic samples and their corresponding tumor cell lines [7]. They identified the genomic alterations and significant amplification of known cancer driver genes, such as *KRAS*, *FGFR2*, *MET*, *ERBB2*, *EGFR*, *MYC*, *CCND1*, and *CD44* in GC with peritoneal metastasis [7]. Among them, the cell surface antigens (FGFR2, MET, HER2, EGFR, and CD44) are potentially treatable with monoclonal antibody (mAb) therapy. Compared to the first four antigens, mAb therapy or diagnosis against CD44 has not been established.

CD44 plays important roles in the tumor progression and has various isoforms, which are generated by the alternative splicing of CD44 mRNA [8]. The mRNA of CD44 standard (CD44s) isoform is produced by constant region exons including the first five (1 to 5) and the last five (16 to 20) [9]. The mRNAs of CD44 variant (CD44v) isoform are produced by the assembling of variant exons (v1–v10) with the constant region exons of CD44s [10]. CD44s and CD44v receive the post-translational modifications, such as *N*-glycosylation and *O*-glycosylation. Therefore, the molecular weight of CD44s is reached 80~100 kDa, and CD44v has various molecular weights (100~250 kDa) due to a variety of glycosylation [11]. Both CD44s and CD44v (pan-CD44) can attach to hyaluronic acid (HA), which is important for cellular adhesion, homing, and motility [12].

CD44v is overexpressed in tumors [13] and promotes tumor malignant progression through the binding to growth factors, and the acquisition of invasiveness, stemness, and drug resistance [14-16]. These were mediated by the unique functions of the variant's exon-encoded region. The v3-encoded region can recruit heparin-binding growth factors to their receptor, and promote the signal transduction [17,18]. The v6-encoded region forms a ternary complex with hepatocyte growth factor and its receptor MET, which is essential for the activation [19]. Furthermore, the v8–10-encoded region binds to and stabilizes a cystine–glutamate transporter (xCT), which enhances cystine uptake and glutathione synthesis [20]. The elevation of reduced glutathione (GSH) mediates the defense to reactive oxygen species (ROS) [20] and chemotherapeutic drugs [21]. The expression of CD44v8–10 is associated with the function of xCT and intracellular redox status, which is associated with the poor prognosis [22]. Therefore, the establishment of CD44v-specific mAbs are essential for CD44-targeting tumor diagnosis and therapy. However, the roles of the variant 8-encoded region in tumor development have not been fully elucidated.

Our group previously established an anti-pan-CD44 mAb, C$_{44}$Mab-5 (IgG$_1$, kappa) [23] using the Cell-Based Immunization and Screening (CBIS) method. Moreover, another anti-pan-CD44 mAb, C$_{44}$Mab-46 [24] was developed by immunizing mice with CD44v3–10 ectodomain. Both C$_{44}$Mab-5 and C$_{44}$Mab-46 have epitopes within the standard exon 2 and 5-encoding regions, respectively [25-27]. We further showed that both C$_{44}$Mab-5 and C$_{44}$Mab-46 are applicable to flow cytometry and immunohistochemical analyses in oral squamous cell carcinomas (OSCC) [23] and esophageal SCC [24]. Furthermore, we produced a class-switched and a defucosylated version of C$_{44}$Mab-5 (5-mG$_{2a}$-f) using fucosyltransferase 8-deficient ExpiCHO-S cells and evaluated the antitumor effects of 5-mG$_{2a}$-f in OSCC xenograft bearing mice [28]. We have developed various anti-CD44v mAbs, including anti-CD44v4 (C$_{44}$Mab-108) [29], anti-CD44v5 (C$_{44}$Mab-3) [30], anti-CD44v6 (C$_{44}$Mab-9) [31], anti-CD44v7/8 (C$_{44}$Mab-34) [32], and anti-CD44v9 (C$_{44}$Mab-1) [33].

In this study, we established a novel anti-CD44v8 mAb, C$_{44}$Mab-94 (IgG$_1$, kappa) using the CBIS method and evaluated its applications.

2. Materials and Methods

2.1. Cell Lines

The human OSCC cell line (HSC-3) and the human gastric cancer cell lines (MKN45 and NUGC-4) were obtained from the Japanese Collection of Research Bioresources (Osaka, Japan). The human pancreatic cancer cell line (PANC-1) was obtained from the Cell Resource Center for Biomedical Research Institute of Development, Aging, and Cancer at Tohoku University (Sendai, Japan). Chinese hamster ovary (CHO)-K1 and P3X63Ag8U.1 (P3U1; a mouse multiple myeloma) cell lines were obtained from the American Type Culture Collection (ATCC, Manassas, VA, USA). HSC-3 was

Preprints (www.preprints.org) | NOT PEER-REVIEWED | Posted: 15 May 2023 doi:10.20944/preprints202305.0995.v1

cultured in DMEM medium (Nacalai Tesque, Inc., Kyoto, Japan), supplemented with 100 μg/mL streptomycin, 100 U/mL penicillin, and 0.25 μg/mL amphotericin B (Nacalai Tesque, Inc.), and 10% (*v*/*v*) heat-inactivated fetal bovine serum (FBS; Thermo Fisher Scientific, Inc., Waltham, MA, USA). The cell lines (MKN45, NUGC-4, PANC-1, CHO-K1, and P3U1) were cultured in RPMI-1640 medium (Nacalai Tesque, Inc.), supplemented as indicated above. All cells were cultured using a humidified incubator at 37°C, in an atmosphere of 5% CO_2 and 95% air.

2.2. Construction of plasmid DNA and Establishment of Stable Transfectants

The cDNAs of CD44s and CD44v3–10 were obtained as described previously [23]. The cDNAs were cloned into pCAG-ssPA16 vectors with a signal sequence and N-terminal PA16 tag (GLEGGVAMPGAEDDVV) [23,34-37], which can be detected by NZ-1 mAb, (anti-human podoplanin [PDPN] mAb） [38-53]. N-terminal PA16-tagged CD44v3–10 deletion mutants (dN224, dN266, dN304, dN343, dN386, dN430, dN464, dN494, and dN562) were amplified using a HotStar HiFidelity Polymerase Kit (Qiagen Inc., Hilden, Germany), and subcloned into the pCAG-ssPA16 vector. The pCAG- ssPA16-CD44s, pCAG-ssPA16-CD44v3–10, and pCAG-ssPA16-CD44v3–10 deletion mutant vectors were transfected into CHO-K1 cells. The pCAG-ssPA16-CD44v3–10 vector was transfected into PANC-1 cells. The transfection was performed using a Neon transfection system (Thermo Fisher Scientific, Inc.). By the limiting dilution method, stable transfectants PANC-1/CD44v3–10, CHO/CD44s, CHO/CD44v3–10, and several deletion mutants of CHO/CD44v3–10 (dN224, dN266, dN304, dN343, dN386, dN430, dN464, dN494, and dN562) were finally established.

2.3. Production of Hybridomas

The 6-week-old female BALB/c mice (CLEA Japan, Tokyo, Japan) were intraperitoneally immunized with PANC-1/CD44v3–10 (1×10^8 cells) and Imject Alum (Thermo Fisher Scientific Inc.). Additional immunizations of PANC-1/CD44v3–10 (1×10^8 cells, three times) and a booster injection of PANC-1/CD44v3–10 (1×10^8 cells) 2 days before the sacrifice were performed. Hybridomas were produced as described previously [30]. The supernatants, which are positive for CHO/CD44v3–10 cells and negative for CHO-K1 cells, were selected by flow cytometry, SA3800 Cell Analyzers (Sony Corp. Tokyo, Japan).

2.4. Enzyme-Linked Immunosorbent Assay (ELISA)

Four peptides, covering from v7, v8, and v9 regions of CD44v3–10, were obtained from Sigma-Aldrich Corp. (St. Louis, MO, USA).

The peptide sequences were as follows.

CD44p421–440 (GHQAGRRMDMDSSHSTTLQP); v7/v8,
CD44p431–450 (DSSHSTTLQPTANPNTGLVE); v8,
CD44p441–460 (TANPNTGLVEDLDRTGPLSM); v8,
CD44p451–470 (DLDRTGPLSMTTQQSNSQSF); v8/v9.

The peptides (10 μg/mL) were immobilized on 96-well immunoplates (Nunc Maxisorp; Thermo Fisher Scientific Inc). The blocking was performed with 1% (*w*/*v*) bovine serum albumin (BSA) in PBST. C_{44}Mab-94 (10 μg/mL) or blocking buffer was added to the peptides-coated wells. The detection was performed as described previously [30].

2.5. Flow Cytometry

In the CBIS screening and epitope mapping, the hybridoma supernatants were treated with CHO-K1, CHO/CD44v3–10, or CHO/CD44v3–10 deletion mutants. In the dose-dependent assay, CHO-K1, CHO/CD44s, CHO/CD44v3–10, MKN45, and NUGC-4 were incubated with C_{44}Mab-94, C_{44}Mab-46, or control blocking buffer (0.1% BSA in PBS). Then, the cells were treated with anti-mouse IgG conjugated with Alexa Fluor 488 (1:2000; Cell Signaling Technology, Inc., Danvers, MA, USA). The data were analyzed using the EC800 Cell Analyzer or the SA3800 Cell Analyzer (Sony Corp.).

 doi:10.20944/preprints202305.0995.v1

2.6. Determination of Dissociation Constant (K_D) by Flow Cytometry

The diluted C_{44}Mab-94 (from 1300 to 0.08 nM) was suspended with CHO/CD44v3–10, MKN45, and NUGC-4 cells. Then, the cells were treated with anti-mouse IgG conjugated with Alexa Fluor 488 (1:200). Fluorescence data were analyzed and the apparent K_D was determined by the fitting binding isotherms to built-in one-site binding models of GraphPad Prism 8 (GraphPad Software, Inc., La Jolla, CA, USA).

2.7. Western Blot Analysis

Cell lysates were prepared as described previously [33], and were denatured in sodium dodecyl sulfate (SDS) sample buffer (Nacalai Tesque, Inc.). The 10 μg of proteins were subjected to electrophoresis using polyacrylamide gels (5–20%; FUJIFILM Wako Pure Chemical Corporation, Osaka, Japan) and transferred onto polyvinylidene difluoride membranes (Merck KGaA, Darmstadt, Germany). The membranes were blocked with 4% skim milk (Nacalai Tesque, Inc.) in PBST, and were incubated with 10 μg/mL of C_{44}Mab-94, 10 μg/mL of C_{44}Mab-46, or 0.5 μg/mL of an anti-β-actin mAb (clone AC-15; Sigma-Aldrich Corp.). The detection was performed as described previously [31].

2.8. Immunohistochemical Analysis

Formalin-fixed paraffin-embedded (FFPE) gastric carcinoma (BS01012e and BS01011b) and OSCC (OR601c) tissue arrays were obtained from US Biomax Inc. (Rockville, MD, USA). The tissue arrays were autoclaved in citrate buffer (pH 6.0; Nichirei Biosciences, Inc., Tokyo, Japan) for 20 min. The blocking was performed using SuperBlock T20 (Thermo Fisher Scientific, Inc.). The sections were incubated with C_{44}Mab-94 (5 μg/mL) and C_{44}Mab-46 (5 μg/mL). The detection was performed as described previously [30].

3. Results

3.1. Establishment of an Anti-CD44v8 mAb, C_{44}Mab-94

We previously used CHO/CD44v3–10 cells as an immunogen and generated anti-CD44 mAbs, including C_{44}Mab-5 (pan-CD44), C_{44}Mab-3 (v5) [30], C_{44}Mab-9 (v6) [31], and C_{44}Mab-1 (v9) [33]. In this study, we newly established a stable transfectant (PANC-1/CD44v3–10 cells) as another immunogen (Figure 1A). Mice were immunized with PANC-1/CD44v3–10 cells (Figure 1B), and hybridomas were seeded in 96-well plates (Figure 1C). The supernatants, which are positive for CHO/CD44v3–10 cells and negative for CHO-K1 cells, were selected using flow cytometry (Figure 1D). After cloning, anti-CD44-mAb-producing clones were finally established. Among established clones, we focused on C_{44}Mab-94 (IgG_1, kappa), and the epitopes were determined by flow cytometry and/or ELISA (Figure 1E).

Preprints (www.preprints.org) | NOT PEER-REVIEWED | Posted: 15 May 2023 doi:10.20944/preprints202305.0995.v1

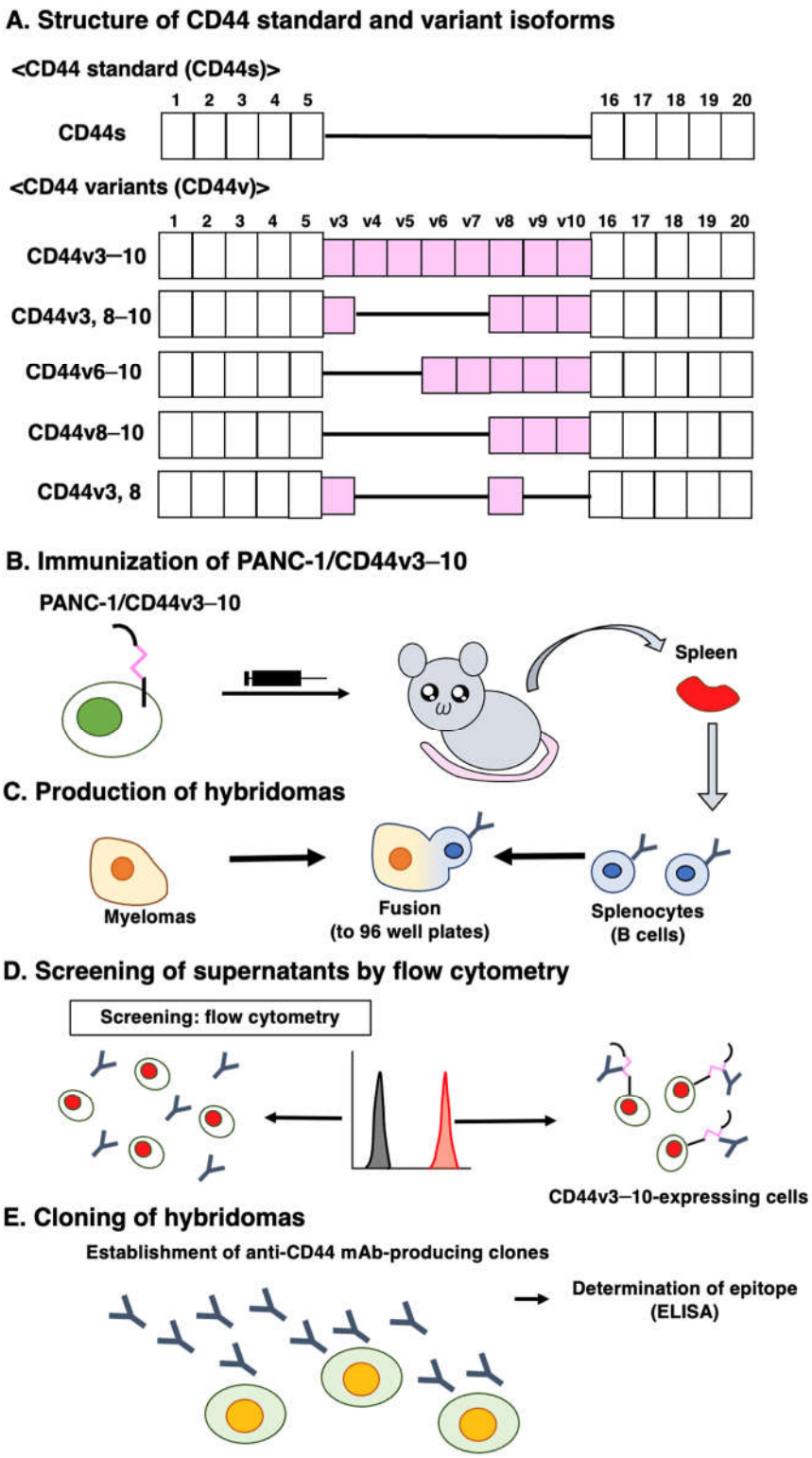

Figure 1. Anti-human CD44 mAbs production. (**A**) The structure of CD44s and CD44v. The mRNA of CD44s is assembled by the constant exons (1–5) and (16–20), and produces the standard isoform, CD44s. The mRNAs of CD44v are generated by the alternative splicing of variant exons. CD44v3–10 is an immunogen. CD44v3, 8–10, CD44v6–10, CD44v8–10, and CD44v3, 8 are detected in GC cell line [54] (**B**) PANC1/CD44v3–10 was used as an immunogen. (**C**) The hybridomas were produced by fusion with splenocytes and P3U1 cells. (**D**) The screening was performed using parental CHO-K1 and CHO/CD44v3–10 cells by flow cytometry. (**E**) A clone C44Mab-94 was established. Furthermore, the binding epitope was determined by flow cytometry using CD44 deletion mutant-expressed CHO-K1 cells and ELISA.

Preprints (www.preprints.org) | NOT PEER-REVIEWED | Posted: 15 May 2023 doi:10.20944/preprints202305.0995.v1

To determine the C44Mab-94 epitope, we examined the reactivity to CHO/CD44v3–10 and the N-terminal CD44v3–10 deletion mutants (dN224, dN266, dN304, dN343, dN386, dN430, dN464, dN494, and dN562)-expressed CHO-K1 cells by flow cytometry (Figure 2A). As shown in Figure 2B, C44Mab-94 reacted with dN224, dN266, dN304, dN343, dN386, dN430, and CD44v3–10. In contrast, the reactivity completely disappeared in dN464, dN494, and dN562. Because CD44v3–10 and the deletion mutants possess PA16 tag at the N-terminus, we could confirm all expression on the cell surface by anti-PA16 tag mAb, NZ-1 (Figure 2C). These results suggest that C44Mab-94 recognizes the v8-encoding sequence.

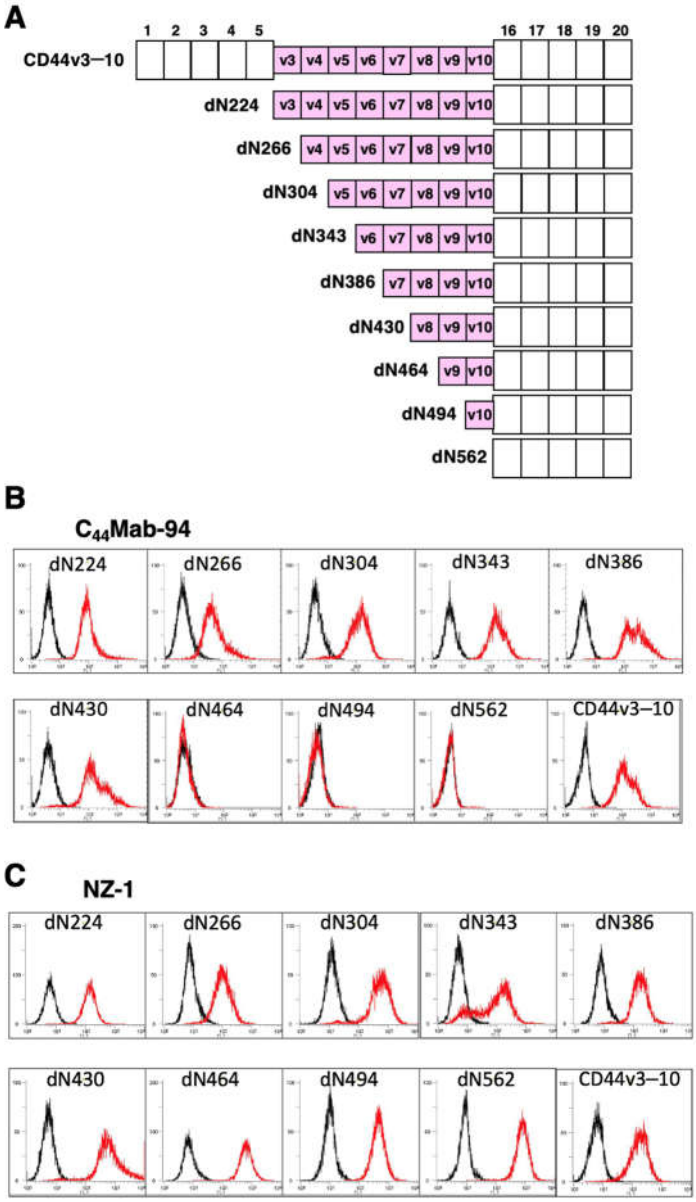

Figure 2. Epitope determination of C44Mab-94 using deletion mutants of CD44v3–10. (**A**) The CD44v3–10 deletion mutants-expressed on CHO-K1 cells. (**B**) The CD44v3–10 mutants-expressed CHO-K1 cells were incubated with C44Mab-94 (**B,** red line) or an anti-PA tag mAb, NZ-1 (**C,** red line), followed by secondary antibodies. The black line represents the negative control (blocking buffer).

To further assess the C44Mab-94 epitope, we performed ELISA using synthetic peptides from the v7- to v9-encoded sequences. As shown in Figure 3, C44Mab-94 reacted with CD44p431–450 (DSSHSTTLQPTANPNTGLVE, v8 region), but not another v8 region (CD44p441–460), v7/v8 region (CD44p421–440), or v8/v9 region (CD44p451–470). These results indicated that C44Mab-94 recognizes the CD44 variant-8-encoded sequence, but not the border sequence between v7 and v8, or v8 and v9.

Preprints (www.preprints.org) | NOT PEER-REVIEWED | Posted: 15 May 2023 doi:10.20944/preprints202305.0995.v1

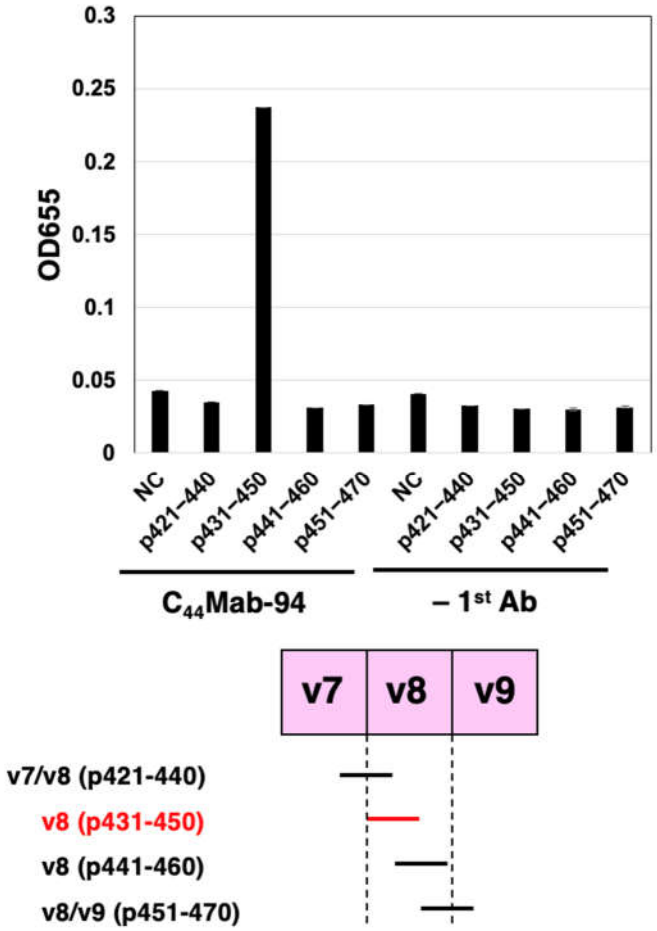

Figure 3 Determination of C44Mab-94 epitope by ELISA. Four synthesized peptides, which cover the CD44v7 to v9 region, were immobilized on immunoplates. The plates were incubated with C44Mab-94 or buffer control (– 1st Ab), followed by incubation with peroxidase-conjugated anti-mouse immunoglobulins. Optical density was measured at 655 nm. NC, negative control (solvent; DMSO in PBS). Error bars represent means ± SDs.

3.2. Flow Cytometric Analysis of C44Mab-94 against CD44-Expressing Cells

We next examined the reactivity of C44Mab-94 against CHO/CD44v3–10 and CHO/CD44s cells by flow cytometry. C44Mab-94 recognized CHO/CD44v3–10 cells in a dose-dependent manner (Figure 4A). In contrast, C44Mab-94 recognized neither CHO/CD44s (Figure 4B) nor CHO-K1 (Figure 4C) cells. We confirmed that a pan-CD44 mAb, C44Mab-46 [24], recognized both CHO/CD44s and CHO/CD44v3–10 cells (Supplementary Figure S1A and B, respectively), but not CHO-K1 cells (Supplementary Figure S1C). Furthermore, C44Mab-94 also recognized the OSCC cell line (HSC-3) and GC cell lines (MKN45, and NUGC-4) in a dose-dependent manner (Figure 4D, E, and F, respectively).

We measured the apparent binding affinity of C44Mab-94 to CHO/CD44v3–10, MKN45, and NUGC-4 cells by flow cytometry. The dissociation constant (K_D) of C44Mab-94 for CHO/CD44v3–10, MKN45, and NUGC-4 was 2.8×10^{-7} M, 3.0×10^{-7} M, and 5.7×10^{-7} M, respectively.

Preprints (www.preprints.org) | NOT PEER-REVIEWED | Posted: 15 May 2023 doi:10.20944/preprints202305.0995.v1

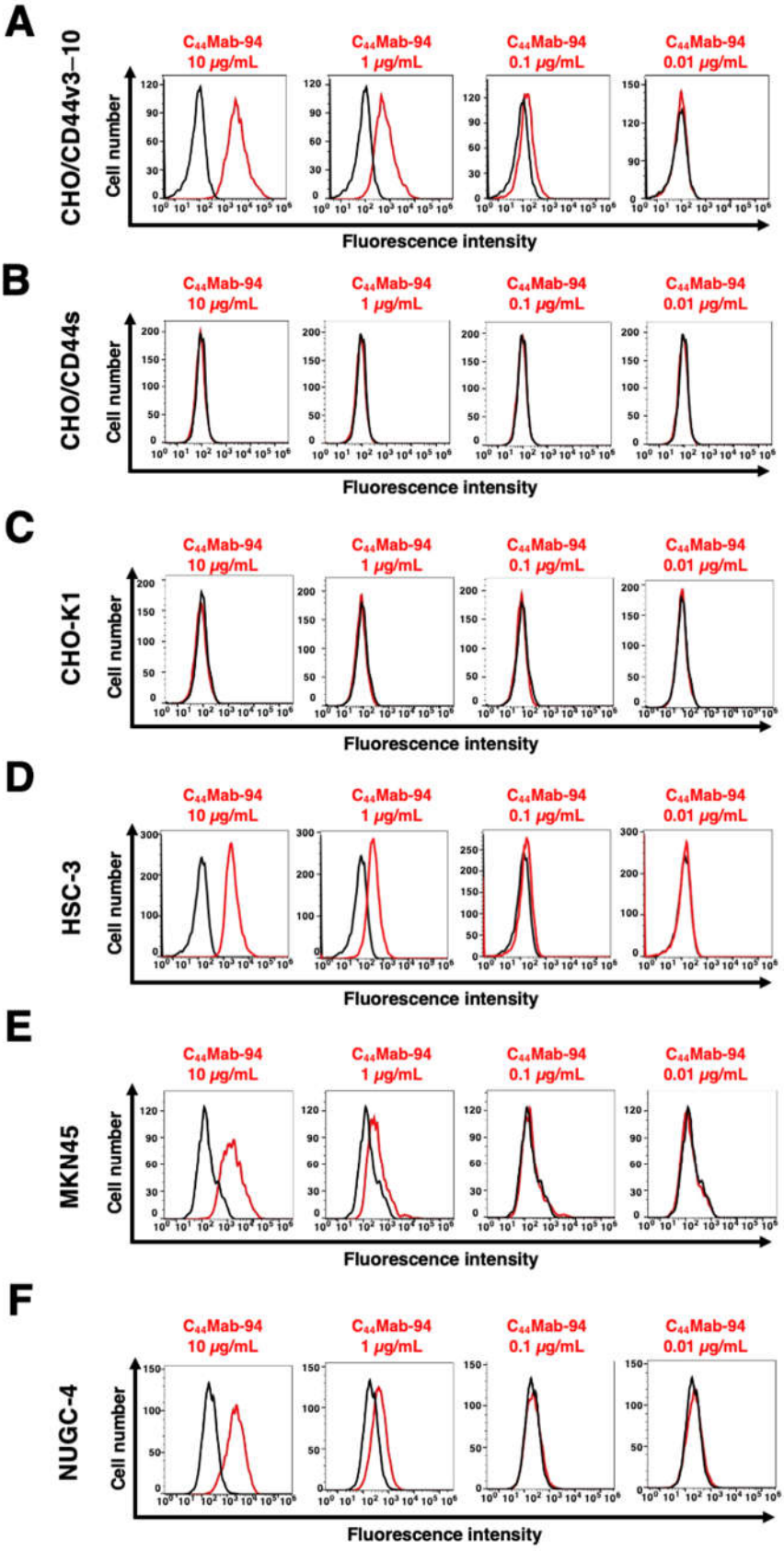

Figure 4. Flow cytometric analysis of C44Mab-94. CHO/CD44v3–10 (**A**), CHO/CD44s (**B**), CHO-K1 (**C**), HSC-3 (**D**), MKN45 (**E**), and NUGC-4 (**F**) cells were incubated with 0.01–10 μg/mL of C44Mab-94. Then, the cells were treated with anti-mouse IgG conjugated with Alexa Fluor 488 (Red line). The black line represents the negative control (blocking buffer).

Preprints (www.preprints.org) | NOT PEER-REVIEWED | Posted: 15 May 2023 doi:10.20944/preprints202305.0995.v1

3.4. Western Blot Analysis

We next conducted western blot analysis to assess the sensitivity of C44Mab-94. Total cell lysates from CHO-K1, CHO/CD44s, CHO/CD44v3–10, HSC-3, MKN45, and NUGC-4 were examined. As shown in Figure 5A, C44Mab-94 detected CD44v3–10 at more than 180-kDa and ~75-kDa bands mainly. Furthermore, C44Mab-94 detected endogenous CD44v8 at more than 100-kDa bands in HSC-3, MKN45, and NUGC-4 cells. An anti-pan-CD44 mAb, C44Mab-46, recognized the lysates from both CHO/CD44s (~75 kDa) and CHO/CD44v3–10 (>180 kDa) (Figure 5B). Although C44Mab-46 strongly recognized the lysates from NUGC-4, the reactivity to the HSC-3 and MKN45 lysates was weak. These results indicated that C44Mab-94 specifically detects exogenous CD44v3–10 and endogenous CD44v8.

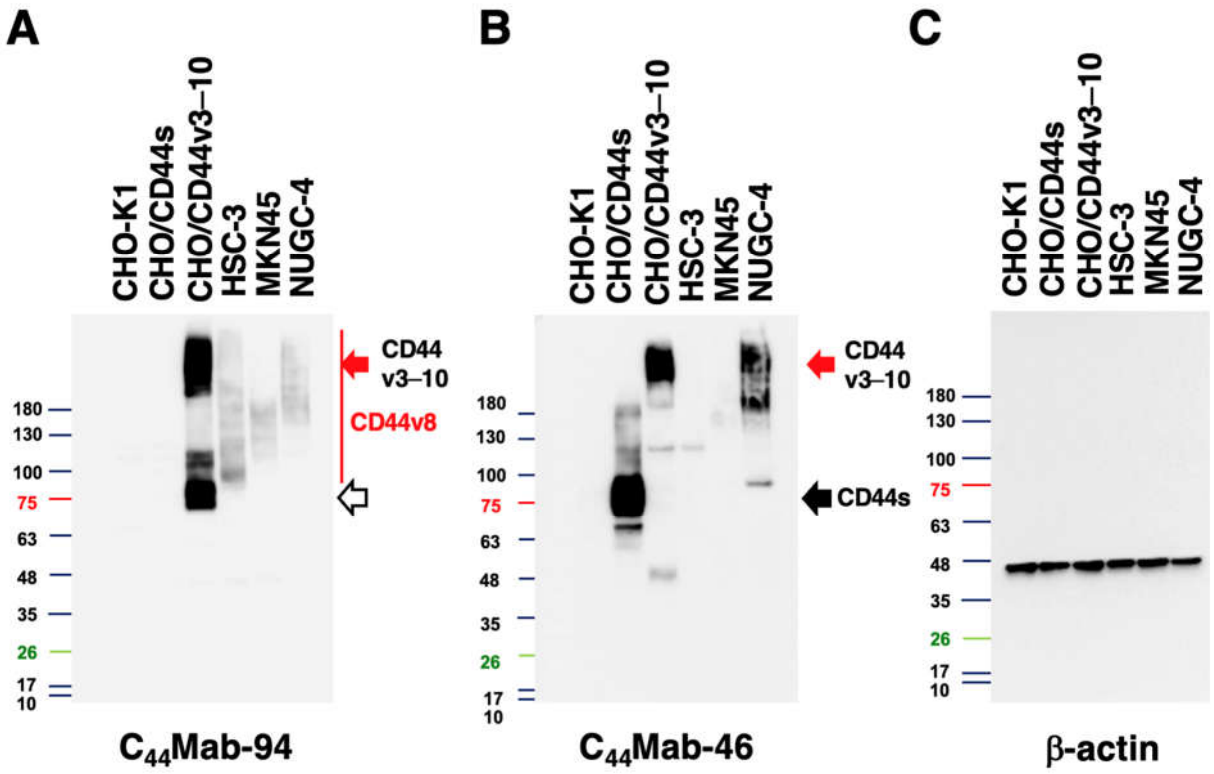

Figure 5. Western blot analysis using C44Mab-94. The cell lysates of CHO-K1, CHO/CD44s, CHO/CD44v3–10, HSC-3, MKN45, and NUGC-4 (10 μg) were electrophoresed and transferred onto polyvinylidene fluoride membranes. The membranes were incubated with 10 μg/mL of C44Mab-94 (**A**), 10 μg/mL of C44Mab-46 (**B**), and 0.5 μg/mL of an anti-β-actin mAb (**C**). Then, the membranes were incubated with anti-mouse immunoglobulins conjugated with peroxidase. The black arrows indicate CD44s (~75 kDa). The red arrows indicate CD44v3–10 (>180 kDa). CD44v8 was broadly detected in HSC-3, MKN45, and NUGC-4 lysates. The white arrow indicates ~75-kDa band recognized by C44Mab-94 in CHO/CD44v3–10 lysate.

3.5. Immunohistochemical Analysis Using C44Mab-94 against Tumor Tissues

We next investigated whether C44Mab-94 could be applied to immunohistochemical analysis using FFPE sections. We first examined the reactivity of C44Mab-94 in the OSCC tissue array because the type was revealed as the second highest CD44-positive cancer type in the Pan-Cancer Atlas [55]. As shown in Supplementary Figure S2A and B, the membranous staining in OSCC was observed by C44Mab-94 and C44Mab-46. In a stromal invaded OSCC section, C44Mab-94 strongly stained invaded OSCC and could clearly distinguish tumor cells from stromal tissues (Supplementary Figure S2C). In contrast, C44Mab-46 stained both invaded OSCC and surrounding stroma cells (Supplementary Figure S2D). Supplementary Table S1 summarized the result of OSCC tissue staining.

Preprints (www.preprints.org) | NOT PEER-REVIEWED | Posted: 15 May 2023 doi:10.20944/preprints202305.0995.v1

We next stained the GC tissue array (BS01011b) using C44Mab-94 and C44Mab-46. C44Mab-94 exhibited membranous staining in IGC (Figure 6A). C44Mab-46 also stained the same type of cancer cells (Figure 6B). Furthermore, membranous and cytoplasmic staining by C44Mab-94 and C44Mab-46 was observed in stromal-invaded tumor cells (Figure 6C and D). In DGC (Figure 6E and F), diffusely spread tumor cells were strongly stained by both C44Mab-94 and C44Mab-46. In contrast, both C44Mab-94 and C44Mab-46 did not stain the ductal epithelial structure of IGC (Figure 6G and H). Additionally, stromal staining by C44Mab-46 was observed in the tissue (Figure 6H).

We summarized the immunohistochemical analysis of GC in Table 1; C44Mab-94 stained 28 out of 72 cases (39%) of GC. A similar staining was also observed in another tissue array (BS01012e, Supplementary Figure S3). We summarized the data of immunohistochemical analysis in Supplementary Table S2. These results indicated that C44Mab-94 is useful to detect CD44v8 in immunohistochemical analysis of FFPE tumor sections.

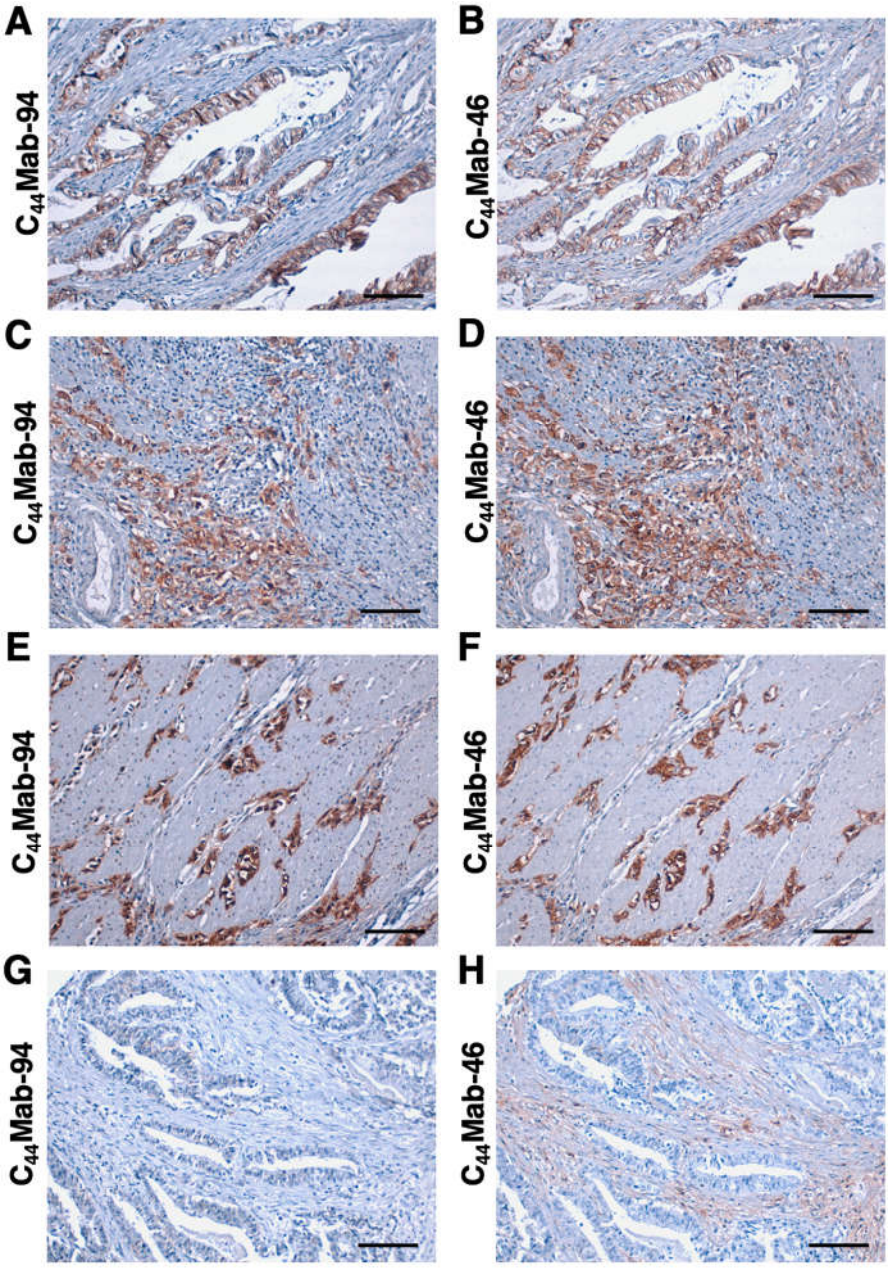

Figure 6. Immunohistochemistry using C44Mab-94 and C44Mab-46 against GC. (**A**–**F**) The serial sections of GC tissue arrays (BS01011b) were treated with 5 μg/mL of C44Mab-94 or 5 μg/mL of C44Mab-46, followed by treatment with the Envision+ kit. The chromogenic reaction was performed using DAB, and the sections were counterstained with hematoxylin. Scale bar = 100 μm.

Preprints (www.preprints.org) | NOT PEER-REVIEWED | Posted: 15 May 2023 doi:10.20944/preprints202305.0995.v1

Table 1. Immunohistochemical analysis using C44Mab-94 and C44Mab-46 against GC tissue array (BS01011b).

No.	Age	Sex	Pathology diagnosis	TNM	Grade	Stage	C44Mab-94	C44Mab-46
1	55	F	Adenocarcinoma	T2N0M0	1	IB	-	+
2	51	F	Adenocarcinoma	T2N0M0	-	IB	-	-
3	71	M	Adenocarcinoma	T3N1M0	1	IIB	-	++
4	63	M	Adenocarcinoma	T3N0M0	1	IIA	-	-
5	61	M	Adenocarcinoma	T2N0M0	1	IB	-	-
6	61	M	Adenocarcinoma	T2N0M0	1	IB	-	+
7	60	M	Adenocarcinoma	T3N2M0	1	IIIA	-	-
8	54	M	Adenocarcinoma	T3N2M0	1	IIIA	+	++
9	46	F	Adenocarcinoma	T3N0M0	1	IIA	-	+
10	66	M	Mucinous adenocarcinoma	T3N0M0	2-3	IIA	-	+
11	56	M	Adenocarcinoma	T2N0M0	2	IB	++	+
12	52	F	Adenocarcinoma	T3N0M0	2	IIA	+	+
13	70	M	Adenocarcinoma	T3N0M0	2	IIA	-	+
14	71	M	Adenocarcinoma	T2N0M0	2	IB	-	++
15	61	M	Adenocarcinoma	T3N0M0	2	IIA	-	-
16	75	M	Adenocarcinoma	T3N1M0	2	IIB	-	-
17	72	F	Adenocarcinoma	T3N0M0	2	IIA	+	+
18	60	M	Adenocarcinoma	T3N0M0	2	IIA	-	-
19	63	F	Adenocarcinoma	T3N0M0	2	IIA	-	-
20	69	M	Adenocarcinoma	T2N0M0	2	IB	-	-
21	54	F	Adenocarcinoma	T3N0M0	2	IIA	-	-
22	50	F	Adenocarcinoma	T3N0M0	3	IIA	-	-
23	64	M	Adenocarcinoma	T3N0M0	3	IIA	-	++
24	59	M	Adenocarcinoma	T2N0M0	2	IB	++	+++
25	59	M	Adenocarcinoma	T2N0M0	2	IB	-	-
26	44	M	Adenocarcinoma	T3N0M0	2	IIA	-	-
27	76	M	Adenocarcinoma	T3N0M0	2	IIA	-	+
28	56	M	Adenocarcinoma	T3N0M0	2	IIA	-	+
29	56	M	Adenocarcinoma	T2N0M0	2	IB	+	+
30	58	M	Adenocarcinoma	T3N0M0	2	IIA	-	+
31	94	M	Adenocarcinoma	T2N0M0	2	IB	+	+
32	56	F	Adenocarcinoma	T2N0M0	3	IB	+	+
33	56	M	Adenocarcinoma	T4N1M0	3	IIIA	+	+
34	51	F	Adenocarcinoma	T3N0M0	2	IIA	+	+
35	67	M	Adenocarcinoma	T3N0M0	2	IIA	+	+
36	53	M	Adenocarcinoma	T3N0M0	2-3	IIA	+	+
37	48	F	Adenocarcinoma	T2N1M0	3	IIA	++	++
38	58	M	Adenocarcinoma	T2N0M0	2	IB	-	-
39	61	M	Adenocarcinoma	T2N0M0	3	IB	-	+

Preprints (www.preprints.org) | NOT PEER-REVIEWED | Posted: 15 May 2023 doi:10.20944/preprints202305.0995.v1

40	62	M	Adenocarcinoma	T2N0M0	3	IB	-	+
41	65	M	Adenocarcinoma	T2N0M0	3	IB	+	+
42	47	F	Adenocarcinoma	T3N1M0	3	IIB	-	-
43	65	M	Adenocarcinoma	T2N0M0	-	IB	-	-
44	52	F	Adenocarcinoma	T2N0M0	3	IB	-	-
45	72	M	Adenocarcinoma	T2N0M0	3	IB	-	+
46	68	F	Adenocarcinoma	T3N0M0	3	IIA	-	++
47	56	M	Adenocarcinoma	T3N0M0	3	IIA	++	++
48	59	M	Adenocarcinoma	T3N1M0	3	IIB	+	+
49	62	M	Adenocarcinoma	T3N1M0	3	IIB	-	-
50	60	M	Adenocarcinoma	T3N1M0	3	IIB	+	+++
51	64	M	Adenocarcinoma	T2N0M0	3	IB	+	+
52	69	M	Adenocarcinoma	T2N0M0	3	IB	+	++
53	75	M	Adenocarcinoma	T2N0M0	3	IB	+	++
54	48	M	Adenocarcinoma	T2N0M0	3	IB	-	-
55	59	M	Adenocarcinoma	T2N0M0	3	IB	-	-
56	64	M	Adenocarcinoma	T3N0M0	3	IIA	+	+
57	55	M	Adenocarcinoma	T2N0M0	3	IB	++	++
58	58	M	Adenocarcinoma	T3N0M0	3	IIA	+	+
59	64	M	Adenocarcinoma	T3N0M0	3	IIA	+	+
60	67	M	Adenocarcinoma	T3N1M0	3	IIB	-	+
61	49	M	Adenocarcinoma	T2N0M0	3	IB	-	-
62	35	M	Adenocarcinoma	T3N1M0	3	IIB	-	-
63	45	F	Adenocarcinoma	T4N0M1	3	IV	+	++
64	43	M	Adenocarcinoma	T2N0M0	3	IB	-	+
65	56	M	Adenocarcinoma	T2N0M0	3	IB	-	-
66	66	M	Adenocarcinoma	T2N0M0	3	IB	+	+
67	60	M	Adenocarcinoma	T3N0M0	3	IIA	-	-
68	74	M	Adenocarcinoma	T2N0M0	3	IB	+	++
69	58	M	Adenocarcinoma	T2N0M0	3	IB	-	-
70	68	M	Mucinous adenocarcinoma	T2N0M0	2	IB	+	+
71	50	M	Mucinous adenocarcinoma	T3N0M0	3	IIA	-	-
72	51	M	Papillary adenocarcinoma	T2N0M0	2	IB	-	+

-, No stain; +, Weak intensity; ++, Moderate intensity; +++, Strong intensity.

4. Discussion

The VFF series anti-CD44v mAbs were previously established by the immunization of bacterial-expressed CD44v3–10 and glutathione *S*-transferase fusion protein [56,57]. The clones, VFF-8 (v5), VFF-18 (v6), VFF-9 (v7), VFF-18(v7/8), and VFF14 (v10) have been used for various applications [58]. Furthermore, VFF18 was humanized as BIWA-4 [59], and developed to bivatuzumab-mertansine, an antibody-drug conjugate (ADC), for clinical trials [60,61]. An anti-CD44v3 mAb (clone 3G5) [62] and an anti-CD44v9 mAb (clone RV3) [20] were also developed and widely used for researches. However, a CD44v8-specific mAb has not been developed.

 doi:10.20944/preprints202305.0995.v1

In this study, we developed a novel anti-CD44v8 mAb, C44Mab-94 using the CBIS method (Figure 1). We determined the epitope as a v8-encoded region using deletion mutants of CD44 (Figure 2), and synthetic peptides (Figure 3). We have established anti-CD44 mAbs using CHO/CD44v3–10 [23,30,31,33], PANC-1/CD44v3–10 (in this study), or purified CD44v3–10 ectodomain [24,32] as antigens. We listed them in our original "Antibody Bank" (see Supplementary Materials). However, clones which recognize the v8-encoded region were rare, suggesting that the region has low antigenicity and/or locates the inside of CD44v3–10 protein. Although the affinity of C44Mab-94 is low against target cells, C44Mab-94 can be applied to various applications, including flow cytometry (Figure 4), western blotting (Figure 5), and immunohistochemistry (Figure 6).

We confirmed that C44Mab-94 recognizes a synthetic peptide of v8-encoded region (DSSHSTTLQPTANPNTGLVE), but not border regions (v7/v8 and v8/v9) by ELISA (Figures 3). The epitope region possesses multiple confirmed and predicted *O*-glycosylation sites [63]. C44Mab-94 recognized a ~75-kDa band in the lysate of CHO/CD44v3–10 (Figure 5A), which is similar to the predicted molecular size from the amino acids of CD44v3–10. Therefore, C44Mab-94 could recognize CD44v3–10 regardless of the glycosylation. The detailed epitope analysis and the influence of glycosylation on C44Mab-94 recognition are requied in future studies.

In a GC cell line, the major transcripts of CD44v, including CD44v3, 8–10, CD44v6–10, CD44v8–10, and CD44v3, 8 were identified [54] (Figure 1A). C44Mab-94 can cover all products of the transcripts, and detect the broad CD44v-expressing GC. Since CD44 v8–10 plays critical roles in the regulation of ROS defense and GC progression [20], an anti-CD44v9 mAb (clone RV3) was mainly used in immunohistochemistry to date. Several studies revealed that CD44v9 is a predictive marker for the recurrence of GC [64] and a biomarker for GC patient selection and efficacy of xCT inhibitors, sulfasalazine [65]. Further investigations are required to reveal the relationship between CD44v8 expression and clinical factors using C44Mab-94. Additionally, C44Mab-94 recognized both IGC (Figure 6A) and DGC (Figure 6E) in immunohistochemistry. It is worthwhile to investigate whether CD44v8 is expressed in a specific molecular subtype of GC [4] in the future study.

A comprehensive analysis of malignant ascites identified the amplifications of cancer driver genes including *CD44* [7]. Although the expression pattern of CD44v is not identified, CD44v8 is thought to be an important target for mAb therapy due to the commonly included region in GC [54]. We have shown the antitumor activity using class-switched and defucosylated IgG2a recombinant mAbs [28,66-72]. The defucosylated IgG2a mAbs can be produced by CHO-K1 lacking fucosyltransferases 8, and exhibited potent ADCC activity *in vitro*, and suppressed the growth of xenograft [28,66-72]. Therefore, the production of defucosylated C44Mab-94 is one of the strategies to evaluate the antitumor effect on GC with peritoneal metastasis in the preclinical model.

Clinical applications of a humanized anti-CD44v6 mAb (BIWA-4) bivatuzumab−mertansine drug conjugate to solid tumors failed because of the skin toxicities [60,61]. The accumulation of mertansine drug was thought to be a cause of the toxicity [60,61]. Human acute myeloid leukemia (AML) cells also express high levels of CD44 mRNA due to suppression of CpG islands methylation in the promoter [73]. Furthermore, higher expression of CD44v6 was observed in AML patients with *FLT3* or *DNMT3A* mutations. Therefore, a mutated version of BIWA-4, called BIWA-8 was engineered to develop chimeric antigen receptors (CARs) for AML. The CD44v6 CAR-T cells exhibited potent anti-leukemic effects [73], indicating that CD44v6 is a rational target of CAR-T therapy for AML harboring *FLT3* or *DNMT3A* mutations. Additionally, the CD44v6 CAR-T also showed an antitumor effect in lung and ovarian cancer xenograft models [74], which is expected for a wider development toward solid tumors.

Because CD44 mRNA is elevated in AML, other CD44 variants could be transcribed in AML. Furthermore, CD44v8–10 was elevated during chronic myeloid leukemia (CML) progression from chronic phase to blast crisis in a humanized mouse model, which is required for the maintenance of stemness of CML [75]. Therefore, we will investigate the reactivity of C44Mab-94 against hematopoietic malignancy. Further studies are required to investigate the selective expression of CD44v8 in leukemia cells, but not in hematopoietic stem cells to certify its safety as a CAR-T antigen.

In this study, we used tumor cell-expressed CD44v3–10 as an immunogen. This strategy is important for the establishment of cancer-specific mAbs (CasMabs). We previously developed

PDPN-targeting CasMabs [76-79] and podocalyxin-targeting CasMabs [80], which recognize cancer-type aberrant glycosylation of the targets [81]. Anti-PDPN-CasMabs are currently applied to CAR-T therapy in preclinical models [48,82,83]. For CasMab development, we should do further screening of our established anti-CD44 mAbs by comparing the reactivity against normal cells. Anti-CD44 CasMabs could be applicable for designing the modalities including ADCs and CAR-T.

Supplementary Materials:

Figure S1, Recognition of CHO/CD44s, CHO/CD44v3–10, and cancer cell lines by C44Mab-46 using flow cytometry.

Figure S2, Immunohistochemistry using C44Mab-94 and C44Mab-46 against OSCC. Figure S3, Immunohistochemistry using C44Mab-94 and C44Mab-46 against GC.

Table S1, Immunohistochemical analysis using C44Mab-94 and C44Mab-46 against OSCC tissue array.

Table S2, Immunohistochemical analysis using C44Mab-94 and C44Mab-46 against GC tissue array (BS01012e).

We listed the information of anti-CD44 mAbs in our original "Antibody Bank" (http://www.med-tohoku-antibody.com/topics/001_paper_antibody_PDIS.htm#CD44 (accessed on 9 May 2023)).

References

1. Sung, H.; Ferlay, J.; Siegel, R.L.; Laversanne, M.; Soerjomataram, I.; Jemal, A.; Bray, F. Global Cancer Statistics 2020: GLOBOCAN Estimates of Incidence and Mortality Worldwide for 36 Cancers in 185 Countries. *CA Cancer J Clin* **2021**, *71*, 209-249, doi:10.3322/caac.21660.
2. Lauren, P. THE TWO HISTOLOGICAL MAIN TYPES OF GASTRIC CARCINOMA: DIFFUSE AND SO-CALLED INTESTINAL-TYPE CARCINOMA. AN ATTEMPT AT A HISTO-CLINICAL CLASSIFICATION. *Acta Pathol Microbiol Scand* **1965**, *64*, 31-49, doi:10.1111/apm.1965.64.1.31.
3. Kushima, R. The updated WHO classification of digestive system tumours-gastric adenocarcinoma and dysplasia. *Pathologe* **2022**, *43*, 8-15, doi:10.1007/s00292-021-01023-7.
4. TheCancerGenomeAtlasResearchNetwork. Comprehensive molecular characterization of gastric adenocarcinoma. *Nature* **2014**, *513*, 202-209, doi:10.1038/nature13480.
5. Shitara, K.; Bang, Y.J.; Iwasa, S.; Sugimoto, N.; Ryu, M.H.; Sakai, D.; Chung, H.C.; Kawakami, H.; Yabusaki, H.; Lee, J.; et al. Trastuzumab Deruxtecan in Previously Treated HER2-Positive Gastric Cancer. *N Engl J Med* **2020**, *382*, 2419-2430, doi:10.1056/NEJMoa2004413.
6. Kang, Y.K.; Boku, N.; Satoh, T.; Ryu, M.H.; Chao, Y.; Kato, K.; Chung, H.C.; Chen, J.S.; Muro, K.; Kang, W.K.; et al. Nivolumab in patients with advanced gastric or gastro-oesophageal junction cancer refractory to, or intolerant of, at least two previous chemotherapy regimens (ONO-4538-12, ATTRACTION-2): a randomised, double-blind, placebo-controlled, phase 3 trial. *Lancet* **2017**, *390*, 2461-2471, doi:10.1016/s0140-6736(17)31827-5.
7. Tanaka, Y.; Chiwaki, F.; Kojima, S.; Kawazu, M.; Komatsu, M.; Ueno, T.; Inoue, S.; Sekine, S.; Matsusaki, K.; Matsushita, H.; et al. Multi-omic profiling of peritoneal metastases in gastric cancer identifies molecular subtypes and therapeutic vulnerabilities. *Nat Cancer* **2021**, *2*, 962-977, doi:10.1038/s43018-021-00240-6.
8. Ponta, H.; Sherman, L.; Herrlich, P.A. CD44: from adhesion molecules to signalling regulators. *Nat Rev Mol Cell Biol* **2003**, *4*, 33-45, doi:10.1038/nrm1004.
9. Yan, Y.; Zuo, X.; Wei, D. Concise Review: Emerging Role of CD44 in Cancer Stem Cells: A Promising Biomarker and Therapeutic Target. *Stem Cells Transl Med* **2015**, *4*, 1033-1043, doi:10.5966/sctm.2015-0048.
10. Chen, C.; Zhao, S.; Karnad, A.; Freeman, J.W. The biology and role of CD44 in cancer progression: therapeutic implications. *J Hematol Oncol* **2018**, *11*, 64, doi:10.1186/s13045-018-0605-5.
11. Mishra, M.N.; Chandavarkar, V.; Sharma, R.; Bhargava, D. Structure, function and role of CD44 in neoplasia. *J Oral Maxillofac Pathol* **2019**, *23*, 267-272, doi:10.4103/jomfp.JOMFP_246_18.
12. Slevin, M.; Krupinski, J.; Gaffney, J.; Matou, S.; West, D.; Delisser, H.; Savani, R.C.; Kumar, S. Hyaluronan-mediated angiogenesis in vascular disease: uncovering RHAMM and CD44 receptor signaling pathways. *Matrix Biol* **2007**, *26*, 58-68, doi:10.1016/j.matbio.2006.08.261.
13. Günthert, U.; Hofmann, M.; Rudy, W.; Reber, S.; Zöller, M.; Haussmann, I.; Matzku, S.; Wenzel, A.; Ponta, H.; Herrlich, P. A new variant of glycoprotein CD44 confers metastatic potential to rat carcinoma cells. *Cell* **1991**, *65*, 13-24, doi:10.1016/0092-8674(91)90403-l.
14. Hassn Mesrati, M.; Syafruddin, S.E.; Mohtar, M.A.; Syahir, A. CD44: A Multifunctional Mediator of Cancer Progression. *Biomolecules* **2021**, *11*, doi:10.3390/biom11121850.

15. Guo, Q.; Yang, C.; Gao, F. The state of CD44 activation in cancer progression and therapeutic targeting. *Febs j* **2021**, doi:10.1111/febs.16179.
16. Zöller, M. CD44: can a cancer-initiating cell profit from an abundantly expressed molecule? *Nat Rev Cancer* **2011**, *11*, 254-267, doi:10.1038/nrc3023.
17. Jackson, D.G.; Bell, J.I.; Dickinson, R.; Timans, J.; Shields, J.; Whittle, N. Proteoglycan forms of the lymphocyte homing receptor CD44 are alternatively spliced variants containing the v3 exon. *J Cell Biol* **1995**, *128*, 673-685, doi:10.1083/jcb.128.4.673.
18. Bennett, K.L.; Jackson, D.G.; Simon, J.C.; Tanczos, E.; Peach, R.; Modrell, B.; Stamenkovic, I.; Plowman, G.; Aruffo, A. CD44 isoforms containing exon V3 are responsible for the presentation of heparin-binding growth factor. *J Cell Biol* **1995**, *128*, 687-698, doi:10.1083/jcb.128.4.687.
19. Orian-Rousseau, V.; Chen, L.; Sleeman, J.P.; Herrlich, P.; Ponta, H. CD44 is required for two consecutive steps in HGF/c-Met signaling. *Genes Dev* **2002**, *16*, 3074-3086, doi:10.1101/gad.242602.
20. Ishimoto, T.; Nagano, O.; Yae, T.; Tamada, M.; Motohara, T.; Oshima, H.; Oshima, M.; Ikeda, T.; Asaba, R.; Yagi, H.; et al. CD44 variant regulates redox status in cancer cells by stabilizing the xCT subunit of system xc(-) and thereby promotes tumor growth. *Cancer Cell* **2011**, *19*, 387-400, doi:10.1016/j.ccr.2011.01.038.
21. Hagiwara, M.; Kikuchi, E.; Tanaka, N.; Kosaka, T.; Mikami, S.; Saya, H.; Oya, M. Variant isoforms of CD44 involves acquisition of chemoresistance to cisplatin and has potential as a novel indicator for identifying a cisplatin-resistant population in urothelial cancer. *BMC Cancer* **2018**, *18*, 113, doi:10.1186/s12885-018-3988-3.
22. Kagami, T.; Yamade, M.; Suzuki, T.; Uotani, T.; Tani, S.; Hamaya, Y.; Iwaizumi, M.; Osawa, S.; Sugimoto, K.; Baba, S.; et al. High expression level of CD44v8-10 in cancer stem-like cells is associated with poor prognosis in esophageal squamous cell carcinoma patients treated with chemoradiotherapy. *Oncotarget* **2018**, *9*, 34876-34888, doi:10.18632/oncotarget.26172.
23. Yamada, S.; Itai, S.; Nakamura, T.; Yanaka, M.; Kaneko, M.K.; Kato, Y. Detection of high CD44 expression in oral cancers using the novel monoclonal antibody, C(44)Mab-5. *Biochem Biophys Rep* **2018**, *14*, 64-68, doi:10.1016/j.bbrep.2018.03.007.
24. Goto, N.; Suzuki, H.; Tanaka, T.; Asano, T.; Kaneko, M.K.; Kato, Y. Development of a Novel Anti-CD44 Monoclonal Antibody for Multiple Applications against Esophageal Squamous Cell Carcinomas. *Int J Mol Sci* **2022**, *23*, doi:10.3390/ijms23105535.
25. Takei, J.; Asano, T.; Suzuki, H.; Kaneko, M.K.; Kato, Y. Epitope Mapping of the Anti-CD44 Monoclonal Antibody (C44Mab-46) Using Alanine-Scanning Mutagenesis and Surface Plasmon Resonance. *Monoclon Antib Immunodiagn Immunother* **2021**, *40*, 219-226, doi:10.1089/mab.2021.0028.
26. Asano, T.; Kaneko, M.K.; Takei, J.; Tateyama, N.; Kato, Y. Epitope Mapping of the Anti-CD44 Monoclonal Antibody (C44Mab-46) Using the REMAP Method. *Monoclon Antib Immunodiagn Immunother* **2021**, *40*, 156-161, doi:10.1089/mab.2021.0012.
27. Asano, T.; Kaneko, M.K.; Kato, Y. Development of a Novel Epitope Mapping System: RIEDL Insertion for Epitope Mapping Method. *Monoclon Antib Immunodiagn Immunother* **2021**, *40*, 162-167, doi:10.1089/mab.2021.0023.
28. Takei, J.; Kaneko, M.K.; Ohishi, T.; Hosono, H.; Nakamura, T.; Yanaka, M.; Sano, M.; Asano, T.; Sayama, Y.; Kawada, M.; et al. A defucosylated antiCD44 monoclonal antibody 5mG2af exerts antitumor effects in mouse xenograft models of oral squamous cell carcinoma. *Oncol Rep* **2020**, *44*, 1949-1960, doi:10.3892/or.2020.7735.
29. Suzuki, H.; Tanaka, T.; Goto, N.; Kaneko, M.K.; Kato, Y. Development of a Novel Anti-CD44 Variant 4 Monoclonal Antibody C44Mab-108 for Immunohistochemistry. *Curr Issues Mol Biol* **2023**, *45*, 1875-1888, doi:10.3390/cimb45030121.
30. Kudo, Y.; Suzuki, H.; Tanaka, T.; Kaneko, M.K.; Kato, Y. Development of a Novel Anti-CD44 variant 5 Monoclonal Antibody C44Mab-3 for Multiple Applications against Pancreatic Carcinomas. *Antibodies* **2023**, *12*, 31, doi:10.3390/antib12020031.
31. Ejima, R.; Suzuki, H.; Tanaka, T.; Asano, T.; Kaneko, M.K.; Kato, Y. Development of a Novel Anti-CD44 Variant 6 Monoclonal Antibody C(44)Mab-9 for Multiple Applications against Colorectal Carcinomas. *Int J Mol Sci* **2023**, *24*, doi:10.3390/ijms24044007.
32. Suzuki, H.; Ozawa, K.; Tanaka, T.; Kaneko, M.K.; Kato, Y. Development of a Novel Anti-CD44 Variant 7/8 Monoclonal Antibody, C44Mab-34, for Multiple Applications against Oral Carcinomas. *Biomedicines* **2023**, *11*, 1099, doi:10.3390/biomedicines11041099.
33. Tawara, M.; Suzuki, H.; Goto, N.; Tanaka, T.; Kaneko, M.K.; Kato, Y. A Novel Anti-CD44 Variant 9 Monoclonal Antibody C44Mab-1 was Developed for Immunohistochemical Analyses Against Colorectal Cancers *Curr. Issues Mol. Biol.* **2023**, *45*, 3658-3673, doi:10.3390/cimb45040238.
34. Kato, Y.; Yamada, S.; Furusawa, Y.; Itai, S.; Nakamura, T.; Yanaka, M.; Sano, M.; Harada, H.; Fukui, M.; Kaneko, M.K. PMab-213: A Monoclonal Antibody for Immunohistochemical Analysis Against Pig Podoplanin. *Monoclon Antib Immunodiagn Immunother* **2019**, *38*, 18-24, doi:10.1089/mab.2018.0048.

35. Furusawa, Y.; Yamada, S.; Itai, S.; Sano, M.; Nakamura, T.; Yanaka, M.; Fukui, M.; Harada, H.; Mizuno, T.; Sakai, Y.; et al. PMab-210: A Monoclonal Antibody Against Pig Podoplanin. *Monoclon Antib Immunodiagn Immunother* **2019**, *38*, 30-36, doi:10.1089/mab.2018.0038.
36. Furusawa, Y.; Yamada, S.; Itai, S.; Nakamura, T.; Yanaka, M.; Sano, M.; Harada, H.; Fukui, M.; Kaneko, M.K.; Kato, Y. PMab-219: A monoclonal antibody for the immunohistochemical analysis of horse podoplanin. *Biochem Biophys Rep* **2019**, *18*, 100616, doi:10.1016/j.bbrep.2019.01.009.
37. Furusawa, Y.; Yamada, S.; Itai, S.; Nakamura, T.; Takei, J.; Sano, M.; Harada, H.; Fukui, M.; Kaneko, M.K.; Kato, Y. Establishment of a monoclonal antibody PMab-233 for immunohistochemical analysis against Tasmanian devil podoplanin. *Biochem Biophys Rep* **2019**, *18*, 100631, doi:10.1016/j.bbrep.2019.100631.
38. Kato, Y.; Kaneko, M.K.; Kuno, A.; Uchiyama, N.; Amano, K.; Chiba, Y.; Hasegawa, Y.; Hirabayashi, J.; Narimatsu, H.; Mishima, K.; et al. Inhibition of tumor cell-induced platelet aggregation using a novel anti-podoplanin antibody reacting with its platelet-aggregation-stimulating domain. *Biochem Biophys Res Commun* **2006**, *349*, 1301-1307, doi:10.1016/j.bbrc.2006.08.171.
39. Chalise, L.; Kato, A.; Ohno, M.; Maeda, S.; Yamamichi, A.; Kuramitsu, S.; Shiina, S.; Takahashi, H.; Ozone, S.; Yamaguchi, J.; et al. Efficacy of cancer-specific anti-podoplanin CAR-T cells and oncolytic herpes virus G47Delta combination therapy against glioblastoma. *Mol Ther Oncolytics* **2022**, *26*, 265-274, doi:10.1016/j.omto.2022.07.006.
40. Ishikawa, A.; Waseda, M.; Ishii, T.; Kaneko, M.K.; Kato, Y.; Kaneko, S. Improved anti-solid tumor response by humanized anti-podoplanin chimeric antigen receptor transduced human cytotoxic T cells in an animal model. *Genes Cells* **2022**, *27*, 549-558, doi:10.1111/gtc.12972.
41. Tamura-Sakaguchi, R.; Aruga, R.; Hirose, M.; Ekimoto, T.; Miyake, T.; Hizukuri, Y.; Oi, R.; Kaneko, M.K.; Kato, Y.; Akiyama, Y.; et al. Moving toward generalizable NZ-1 labeling for 3D structure determination with optimized epitope-tag insertion. *Acta Crystallogr D Struct Biol* **2021**, *77*, 645-662, doi:10.1107/S2059798321002527.
42. Kaneko, M.K.; Ohishi, T.; Nakamura, T.; Inoue, H.; Takei, J.; Sano, M.; Asano, T.; Sayama, Y.; Hosono, H.; Suzuki, H.; et al. Development of Core-Fucose-Deficient Humanized and Chimeric Anti-Human Podoplanin Antibodies. *Monoclon Antib Immunodiagn Immunother* **2020**, *39*, 167-174, doi:10.1089/mab.2020.0019.
43. Fujii, Y.; Matsunaga, Y.; Arimori, T.; Kitago, Y.; Ogasawara, S.; Kaneko, M.K.; Kato, Y.; Takagi, J. Tailored placement of a turn-forming PA tag into the structured domain of a protein to probe its conformational state. *J Cell Sci* **2016**, *129*, 1512-1522, doi:10.1242/jcs.176685.
44. Abe, S.; Kaneko, M.K.; Tsuchihashi, Y.; Izumi, T.; Ogasawara, S.; Okada, N.; Sato, C.; Tobiume, M.; Otsuka, K.; Miyamoto, L.; et al. Antitumor effect of novel anti-podoplanin antibody NZ-12 against malignant pleural mesothelioma in an orthotopic xenograft model. *Cancer Sci* **2016**, *107*, 1198-1205, doi:10.1111/cas.12985.
45. Kaneko, M.K.; Abe, S.; Ogasawara, S.; Fujii, Y.; Yamada, S.; Murata, T.; Uchida, H.; Tahara, H.; Nishioka, Y.; Kato, Y. Chimeric Anti-Human Podoplanin Antibody NZ-12 of Lambda Light Chain Exerts Higher Antibody-Dependent Cellular Cytotoxicity and Complement-Dependent Cytotoxicity Compared with NZ-8 of Kappa Light Chain. *Monoclon Antib Immunodiagn Immunother* **2017**, *36*, 25-29, doi:10.1089/mab.2016.0047.
46. Ito, A.; Ohta, M.; Kato, Y.; Inada, S.; Kato, T.; Nakata, S.; Yatabe, Y.; Goto, M.; Kaneda, N.; Kurita, K.; et al. A Real-Time Near-Infrared Fluorescence Imaging Method for the Detection of Oral Cancers in Mice Using an Indocyanine Green-Labeled Podoplanin Antibody. *Technol Cancer Res Treat* **2018**, *17*, 1533033818767936, doi:10.1177/1533033818767936.
47. Tamura, R.; Oi, R.; Akashi, S.; Kaneko, M.K.; Kato, Y.; Nogi, T. Application of the NZ-1 Fab as a crystallization chaperone for PA tag-inserted target proteins. *Protein Sci* **2019**, *28*, 823-836, doi:10.1002/pro.3580.
48. Shiina, S.; Ohno, M.; Ohka, F.; Kuramitsu, S.; Yamamichi, A.; Kato, A.; Motomura, K.; Tanahashi, K.; Yamamoto, T.; Watanabe, R.; et al. CAR T Cells Targeting Podoplanin Reduce Orthotopic Glioblastomas in Mouse Brains. *Cancer Immunol Res* **2016**, *4*, 259-268, doi:10.1158/2326-6066.Cir-15-0060.
49. Kuwata, T.; Yoneda, K.; Mori, M.; Kanayama, M.; Kuroda, K.; Kaneko, M.K.; Kato, Y.; Tanaka, F. Detection of Circulating Tumor Cells (CTCs) in Malignant Pleural Mesothelioma (MPM) with the "Universal" CTC-Chip and An Anti-Podoplanin Antibody NZ-1.2. *Cells* **2020**, *9*, doi:10.3390/cells9040888.
50. Nishinaga, Y.; Sato, K.; Yasui, H.; Taki, S.; Takahashi, K.; Shimizu, M.; Endo, R.; Koike, C.; Kuramoto, N.; Nakamura, S.; et al. Targeted Phototherapy for Malignant Pleural Mesothelioma: Near-Infrared Photoimmunotherapy Targeting Podoplanin. *Cells* **2020**, *9*, doi:10.3390/cells9041019.
51. Fujii, Y.; Kaneko, M.; Neyazaki, M.; Nogi, T.; Kato, Y.; Takagi, J. PA tag: a versatile protein tagging system using a super high affinity antibody against a dodecapeptide derived from human podoplanin. *Protein Expr Purif* **2014**, *95*, 240-247, doi:10.1016/j.pep.2014.01.009.

52. Kato, Y.; Kaneko, M.K.; Kunita, A.; Ito, H.; Kameyama, A.; Ogasawara, S.; Matsuura, N.; Hasegawa, Y.; Suzuki-Inoue, K.; Inoue, O.; et al. Molecular analysis of the pathophysiological binding of the platelet aggregation-inducing factor podoplanin to the C-type lectin-like receptor CLEC-2. *Cancer Sci* **2008**, *99*, 54-61, doi:10.1111/j.1349-7006.2007.00634.x.
53. Kato, Y.; Vaidyanathan, G.; Kaneko, M.K.; Mishima, K.; Srivastava, N.; Chandramohan, V.; Pegram, C.; Keir, S.T.; Kuan, C.T.; Bigner, D.D.; et al. Evaluation of anti-podoplanin rat monoclonal antibody NZ-1 for targeting malignant gliomas. *Nucl Med Biol* **2010**, *37*, 785-794, doi:10.1016/j.nucmedbio.2010.03.010.
54. Qiu, S.; Iimori, M.; Edahiro, K.; Fujimoto, Y.; Matsuoka, K.; Oki, E.; Maehara, Y.; Mori, M.; Kitao, H. CD44v3,8-10 is essential for Slug-dependent vimentin gene expression to acquire TGF-β1-induced tumor cell motility. *Cancer Sci* **2022**, *113*, 2654-2667, doi:10.1111/cas.15353.
55. Ludwig, N.; Szczepanski, M.J.; Gluszko, A.; Szafarowski, T.; Azambuja, J.H.; Dolg, L.; Gellrich, N.C.; Kampmann, A.; Whiteside, T.L.; Zimmerer, R.M. CD44(+) tumor cells promote early angiogenesis in head and neck squamous cell carcinoma. *Cancer Lett* **2019**, *467*, 85-95, doi:10.1016/j.canlet.2019.10.010.
56. Heider, K.H.; Sproll, M.; Susani, S.; Patzelt, E.; Beaumier, P.; Ostermann, E.; Ahorn, H.; Adolf, G.R. Characterization of a high-affinity monoclonal antibody specific for CD44v6 as candidate for immunotherapy of squamous cell carcinomas. *Cancer Immunol Immunother* **1996**, *43*, 245-253, doi:10.1007/s002620050329.
57. Heider, K.H.; Mulder, J.W.; Ostermann, E.; Susani, S.; Patzelt, E.; Pals, S.T.; Adolf, G.R. Splice variants of the cell surface glycoprotein CD44 associated with metastatic tumour cells are expressed in normal tissues of humans and cynomolgus monkeys. *Eur J Cancer* **1995**, *31a*, 2385-2391, doi:10.1016/0959-8049(95)00420-3.
58. Gansauge, F.; Gansauge, S.; Zobywalski, A.; Scharnweber, C.; Link, K.H.; Nussler, A.K.; Beger, H.G. Differential expression of CD44 splice variants in human pancreatic adenocarcinoma and in normal pancreas. *Cancer Res* **1995**, *55*, 5499-5503.
59. Verel, I.; Heider, K.H.; Siegmund, M.; Ostermann, E.; Patzelt, E.; Sproll, M.; Snow, G.B.; Adolf, G.R.; van Dongen, G.A. Tumor targeting properties of monoclonal antibodies with different affinity for target antigen CD44V6 in nude mice bearing head-and-neck cancer xenografts. *Int J Cancer* **2002**, *99*, 396-402, doi:10.1002/ijc.10369.
60. Riechelmann, H.; Sauter, A.; Golze, W.; Hanft, G.; Schroen, C.; Hoermann, K.; Erhardt, T.; Gronau, S. Phase I trial with the CD44v6-targeting immunoconjugate bivatuzumab mertansine in head and neck squamous cell carcinoma. *Oral Oncol* **2008**, *44*, 823-829, doi:10.1016/j.oraloncology.2007.10.009.
61. Tijink, B.M.; Buter, J.; de Bree, R.; Giaccone, G.; Lang, M.S.; Staab, A.; Leemans, C.R.; van Dongen, G.A. A phase I dose escalation study with anti-CD44v6 bivatuzumab mertansine in patients with incurable squamous cell carcinoma of the head and neck or esophagus. *Clin Cancer Res* **2006**, *12*, 6064-6072, doi:10.1158/1078-0432.Ccr-06-0910.
62. Fox, S.B.; Fawcett, J.; Jackson, D.G.; Collins, I.; Gatter, K.C.; Harris, A.L.; Gearing, A.; Simmons, D.L. Normal human tissues, in addition to some tumors, express multiple different CD44 isoforms. *Cancer Res* **1994**, *54*, 4539-4546.
63. Mereiter, S.; Martins Á, M.; Gomes, C.; Balmaña, M.; Macedo, J.A.; Polom, K.; Roviello, F.; Magalhães, A.; Reis, C.A. O-glycan truncation enhances cancer-related functions of CD44 in gastric cancer. *FEBS Lett* **2019**, *593*, 1675-1689, doi:10.1002/1873-3468.13432.
64. Hirata, K.; Suzuki, H.; Imaeda, H.; Matsuzaki, J.; Tsugawa, H.; Nagano, O.; Asakura, K.; Saya, H.; Hibi, T. CD44 variant 9 expression in primary early gastric cancer as a predictive marker for recurrence. *Br J Cancer* **2013**, *109*, 379-386, doi:10.1038/bjc.2013.314.
65. Shitara, K.; Doi, T.; Nagano, O.; Imamura, C.K.; Ozeki, T.; Ishii, Y.; Tsuchihashi, K.; Takahashi, S.; Nakajima, T.E.; Hironaka, S.; et al. Dose-escalation study for the targeting of CD44v(+) cancer stem cells by sulfasalazine in patients with advanced gastric cancer (EPOC1205). *Gastric Cancer* **2017**, *20*, 341-349, doi:10.1007/s10120-016-0610-8.
66. Li, G.; Suzuki, H.; Ohishi, T.; Asano, T.; Tanaka, T.; Yanaka, M.; Nakamura, T.; Yoshikawa, T.; Kawada, M.; Kaneko, M.K.; et al. Antitumor activities of a defucosylated anti-EpCAM monoclonal antibody in colorectal carcinoma xenograft models. *Int J Mol Med* **2023**, *51*, doi:10.3892/ijmm.2023.5221.
67. Nanamiya, R.; Takei, J.; Ohishi, T.; Asano, T.; Tanaka, T.; Sano, M.; Nakamura, T.; Yanaka, M.; Handa, S.; Tateyama, N.; et al. Defucosylated Anti-Epidermal Growth Factor Receptor Monoclonal Antibody (134-mG(2a)-f) Exerts Antitumor Activities in Mouse Xenograft Models of Canine Osteosarcoma. *Monoclon Antib Immunodiagn Immunother* **2022**, *41*, 1-7, doi:10.1089/mab.2021.0036.
68. Kawabata, H.; Suzuki, H.; Ohishi, T.; Kawada, M.; Kaneko, M.K.; Kato, Y. A Defucosylated Mouse Anti-CD10 Monoclonal Antibody (31-mG(2a)-f) Exerts Antitumor Activity in a Mouse Xenograft Model of CD10-Overexpressed Tumors. *Monoclon Antib Immunodiagn Immunother* **2022**, *41*, 59-66, doi:10.1089/mab.2021.0048.
69. Kawabata, H.; Ohishi, T.; Suzuki, H.; Asano, T.; Kawada, M.; Suzuki, H.; Kaneko, M.K.; Kato, Y. A Defucosylated Mouse Anti-CD10 Monoclonal Antibody (31-mG(2a)-f) Exerts Antitumor Activity in a

Mouse Xenograft Model of Renal Cell Cancers. *Monoclon Antib Immunodiagn Immunother* **2022**, doi:10.1089/mab.2021.0049.

70. Asano, T.; Tanaka, T.; Suzuki, H.; Li, G.; Ohishi, T.; Kawada, M.; Yoshikawa, T.; Kaneko, M.K.; Kato, Y. A Defucosylated Anti-EpCAM Monoclonal Antibody (EpMab-37-mG(2a)-f) Exerts Antitumor Activity in Xenograft Model. *Antibodies (Basel)* **2022**, *11*, doi:10.3390/antib11040074.
71. Tateyama, N.; Nanamiya, R.; Ohishi, T.; Takei, J.; Nakamura, T.; Yanaka, M.; Hosono, H.; Saito, M.; Asano, T.; Tanaka, T.; et al. Defucosylated Anti-Epidermal Growth Factor Receptor Monoclonal Antibody 134-mG(2a)-f Exerts Antitumor Activities in Mouse Xenograft Models of Dog Epidermal Growth Factor Receptor-Overexpressed Cells. *Monoclon Antib Immunodiagn Immunother* **2021**, *40*, 177-183, doi:10.1089/mab.2021.0022.
72. Takei, J.; Ohishi, T.; Kaneko, M.K.; Harada, H.; Kawada, M.; Kato, Y. A defucosylated anti-PD-L1 monoclonal antibody 13-mG(2a)-f exerts antitumor effects in mouse xenograft models of oral squamous cell carcinoma. *Biochem Biophys Rep* **2020**, *24*, 100801, doi:10.1016/j.bbrep.2020.100801.
73. Tang, L.; Huang, H.; Tang, Y.; Li, Q.; Wang, J.; Li, D.; Zhong, Z.; Zou, P.; You, Y.; Cao, Y.; et al. CD44v6 chimeric antigen receptor T cell specificity towards AML with FLT3 or DNMT3A mutations. *Clin Transl Med* **2022**, *12*, e1043, doi:10.1002/ctm2.1043.
74. Porcellini, S.; Asperti, C.; Corna, S.; Cicoria, E.; Valtolina, V.; Stornaiuolo, A.; Valentinis, B.; Bordignon, C.; Traversari, C. CAR T Cells Redirected to CD44v6 Control Tumor Growth in Lung and Ovary Adenocarcinoma Bearing Mice. *Front Immunol* **2020**, *11*, 99, doi:10.3389/fimmu.2020.00099.
75. Holm, F.; Hellqvist, E.; Mason, C.N.; Ali, S.A.; Delos-Santos, N.; Barrett, C.L.; Chun, H.J.; Minden, M.D.; Moore, R.A.; Marra, M.A.; et al. Reversion to an embryonic alternative splicing program enhances leukemia stem cell self-renewal. *Proc Natl Acad Sci U S A* **2015**, *112*, 15444-15449, doi:10.1073/pnas.1506943112.
76. Kato, Y.; Kaneko, M.K. A cancer-specific monoclonal antibody recognizes the aberrantly glycosylated podoplanin. *Sci Rep* **2014**, *4*, 5924, doi:10.1038/srep05924.
77. Kaneko, M.K.; Nakamura, T.; Kunita, A.; Fukayama, M.; Abe, S.; Nishioka, Y.; Yamada, S.; Yanaka, M.; Saidoh, N.; Yoshida, K.; et al. ChLpMab-23: Cancer-Specific Human-Mouse Chimeric Anti-Podoplanin Antibody Exhibits Antitumor Activity via Antibody-Dependent Cellular Cytotoxicity. *Monoclon Antib Immunodiagn Immunother* **2017**, *36*, 104-112, doi:10.1089/mab.2017.0014.
78. Kaneko, M.K.; Yamada, S.; Nakamura, T.; Abe, S.; Nishioka, Y.; Kunita, A.; Fukayama, M.; Fujii, Y.; Ogasawara, S.; Kato, Y. Antitumor activity of chLpMab-2, a human-mouse chimeric cancer-specific antihuman podoplanin antibody, via antibody-dependent cellular cytotoxicity. *Cancer Med* **2017**, *6*, 768-777, doi:10.1002/cam4.1049.
79. Suzuki, H.; Kaneko, M.K.; Kato, Y. Roles of Podoplanin in Malignant Progression of Tumor. *Cells* **2022**, *11*, 575, doi:10.3390/cells11030575.
80. Kaneko, M.K.; Ohishi, T.; Kawada, M.; Kato, Y. A cancer-specific anti-podocalyxin monoclonal antibody (60-mG(2a)-f) exerts antitumor effects in mouse xenograft models of pancreatic carcinoma. *Biochem Biophys Rep* **2020**, *24*, 100826, doi:10.1016/j.bbrep.2020.100826.
81. Suzuki, H.; Kaneko, M.K.; Kato, Y. Roles of Podoplanin in Malignant Progression of Tumor. *Cells* **2022**, *11*, doi:10.3390/cells11030575.
82. Ishikawa, A.; Waseda, M.; Ishii, T.; Kaneko, M.K.; Kato, Y.; Kaneko, S. Improved anti-solid tumor response by humanized anti-podoplanin chimeric antigen receptor transduced human cytotoxic T cells in an animal model. *Genes Cells* **2022**, 9, 549-558, doi:10.1111/gtc.12972.
83. Chalise, L.; Kato, A.; Ohno, M.; Maeda, S.; Yamamichi, A.; Kuramitsu, S.; Shiina, S.; Takahashi, H.; Ozone, S.; Yamaguchi, J.; et al. Efficacy of cancer-specific anti-podoplanin CAR-T cells and oncolytic herpes virus G47Δ combination therapy against glioblastoma. *Molecular Therapy - Oncolytics* **2022**, *26*, 265-274, doi:https://doi.org/10.1016/j.omto.2022.07.006.